
FUDGE: A HIGH-BANDWIDTH FUSION DIAGNOSTIC FOR THE NATIONAL IGNITION FACILITY

M. J. Moran

Introduction

The fusion diagnostic gamma-ray experiment (FUDGE), essentially a magnetic Compton spectrometer combined with a Cherenkov detector, is a high-bandwidth fusion diagnostic for the National Ignition Facility (NIF). Nuclear diagnostics will play a critical role in the success of future inertial confinement fusion (ICF) experiments at the NIF. Diagnostics must go beyond measurement of fusion yield to characterizing details of the fusion burn. Imaging and temporal measurements are important because they provide data for comparison with theoretical predictions. The comparisons show how details of fusion behavior depend on target and experiment design. These data will serve as the basis of an iterative process of design and experiment that will lead to optimization of fusion performance.

Neutron and x-ray images are important for understanding how to compress an ICF target to the desired size and shape. Images provide a direct indication of the integrity of the compressed target during the fusion burn. Such data can give clear indications of high-quality performance and can also provide evidence of imperfect target compression in unsuccessful experiments. Image data go far beyond indications of success or failure by indicating how the spatial distributions of the source might be related to performance in experiments. These results can suggest specific approaches for improving performance for subsequent experiments.

Burn-history measurements of emission rate can serve as indicators of the instantaneous source temperature and other details of behavior that are not evident in time-integrated images. In addition to following the instantaneous reaction rate, the data are highly sensitive to instantaneous temperature (rate $\propto T^5$). When compared with images, the reaction rate can be used to

infer source temperature, or to provide independent indication of unexpected behavior. Again, as with images, time-dependent behavior can help to suggest approaches for improving system performance.

The NIF will require new burn-history diagnostics because the techniques that have been used traditionally will no longer be feasible. The relatively low fusion yields of previous experiments have made it possible to place detector components a few centimeters from the source, where temporal dispersion of neutron signals can be small.¹ In addition, streak cameras could be located a few tens of centimeters from the source without suffering serious radiation damage. At the NIF, physical constraints and high radiation doses in the target chamber will force diagnostic components to be located at distances of the order of meters from the source, where temporal broadening of neutron signals will mask the source pulse shape.

Gamma-Ray Diagnostics

One promising approach to burn-history measurements at the NIF is with diagnostics based on the 16.7-MeV γ ray associated with (D,T) fusion. This γ ray is ideal for measuring (D,T) fusion reaction rates because it is free of the temporal dispersion that frustrates neutron-based measurements. The presence of this γ ray is well known, although associated spectrum and “branching ratio” have proven difficult to measure accurately. The most recent measurement finds for ${}^3\text{H}(\text{d},\gamma){}^5\text{He}/{}^3\text{H}(\text{d},\alpha)\text{n}$ a branching ratio of 1.2×10^{-4} , with the γ rays in two broad lines at 11.5 (FWHM ≈ 7 MeV) and 16.7 (FWHM ≈ 2 MeV) MeV (Ref. 2). This result is within the range of 2×10^{-5} to 3×10^{-4} that had been reported in previous measurements. The rather small branching ratio means that γ -ray measurements of (D,T) fusion reaction rates are practical only for intense short-pulse experiments. For weaker sources, neutron

backgrounds make it extremely difficult to extract the desired γ -ray signal.

Several approaches have been used previously for designing a fusion γ -ray diagnostic. Filtered and heavily shielded scintillation detectors have been used in tokamak experiments.³ Cherenkov detectors and gas-Cherenkov detectors have been discussed, sometimes in tandem with magnetic Compton spectrometers.^{4,5,6} These attempts were often frustrated by small signals in the presence of large neutron backgrounds. With the large emission rates anticipated for NIF experiments, it becomes possible to choose a γ -ray diagnostic design having an excellent signal-to-background ratio with high-bandwidth signal recording.

Three basic considerations constrain the design of a fusion γ -ray diagnostic: (1) the instrument should provide sufficient energy discrimination to eliminate signals from lower-energy γ rays generated by $(n,n'\gamma)$ and other nuclear reactions; (2) the diagnostic also must feature some form of energy dispersion, as the spectral resolution must be achieved in single-shot measurements; and (3) the detector should be fast and have sufficient sensitivity to measure the rays. These requirements can be met by a magnetic Compton spectrometer with a Cherenkov detector (i.e., the FUDGE).

In a Compton spectrometer, γ rays scatter electrons from a (γ,e^-) converter target. The recoil electrons, after energy selection in a sector magnet, are detected in a high-gain, high-bandwidth Cherenkov detector. The three components—the (γ,e^-) converter, the sector magnet, and the Cherenkov detector—can be designed for optimum performance from the overall system.

The (γ,e^-) converter, although very simple, offers choices with respect to scattering cross section and type of material. At a first glance, the rather large total cross section associated with pair production would suggest that thin, high- Z targets be used as the converter (Z is the atomic number of the target material). However, multiple scattering, energy loss, and loss of spectral signature are significant disadvantages for pair production. Pair production increases with Z^2 , but so does multiple scattering. Energy loss in dense, high- Z materials compounds the undesirable effects of multiple scattering. The flat energy spectrum of electrons from pair production reduces the benefits that might be obtained from spectral resolution.

Compton Scattering

Compton scattering is a (γ,e^-) converter mechanism that, despite its smaller total cross section, lends itself nicely to a fusion- γ diagnostic. The differential cross section (i.e., the Klein–Nishina formula) peaks in the forward direction with an angular width of about $1/E\gamma$. For 16.7-MeV γ rays, the majority of the recoil electrons are in a narrow (width $\approx 3^\circ$), forward-directed cone

with energies near that of the original γ ray. Thick, low- Z Compton converters maximize the conversion efficiency while minimizing the effects of multiple scattering.

Figure 1 shows a comparison of (γ,e^-) conversion for 16.7-MeV photons in targets that optimize the efficiency for pair production and Compton scattering. The pair-production target is 0.5 mm of Pb, while the Compton target is 5 mm of Be. The distributions are calculated with the Gluckstern et al.⁷ formulation for pair production and the Klein–Nishina formula⁸ for Compton scattering. In the model used here, the targets are divided into about ten thin layers. Electrons scattered from individual layers are transported, with energy loss⁹ and multiple scattering¹⁰ used to estimate contributions to the overall conversion flux from the converter. The distribution has 0.5-MeV energy increments and 3° angular bins.

The results show that the larger total cross section of pair production produces a distribution that cannot be collected efficiently either in space or in energy. The total cross section for Compton scattering, although about 16 times smaller, is directed into a narrow beam with good energy definition. The forward-directed peak is about twice as intense as the pair-production peak. Thus, in a diagnostic where good energy discrimination and well defined trajectories are required, Compton scattering is the desirable choice.

Magnetic Analysis

The recoil electron beam must be collected and energy analyzed efficiently in order to achieve good performance. This function is accomplished with a

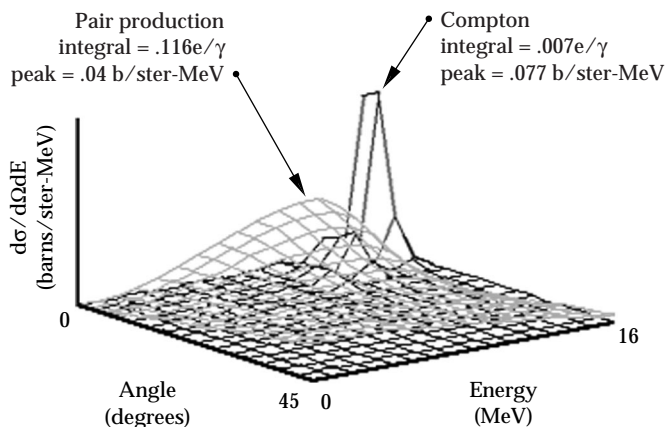


FIGURE 1. Scattered electron distribution from 0.5 mm of Pb compared with that from 5 mm of Be. The Pb, with higher Z , has a larger total cross section from pair production and greater elastic scattering. Compton scattering in the Be, with similar electron areal density, emphasizes forward scattering in a peak with good energy definition. (08-00-1198-2237pb01)

sector-magnet dipole.⁴ With a deflection angle of 30° , spectral dispersion can isolate the desired broad band at about 16 MeV. The deflection trajectories also function as a collecting lens. With slight non-normal incidence on the magnet, the magnet functions as a cylindrical lens in the vertical direction. Figure 2 illustrates the electron optics of the system.

This compact design has sufficient energy resolution to collect the desired electron energies, while rejecting lower-energy electrons strongly. Figure 2 shows that 8-MeV electrons will be very strongly deflected, and electrons with still lower energies will be unable to exit the magnet assembly. Because most of the photon background will have energies below 8 MeV, the magnet will be an effective background shield.

System Performance

The data in Figure 1 can be used to estimate the overall (γ, e^-) Compton conversion efficiency. Assuming a converter with an area of 2 cm^2 located 2.5 m from the source, the solid-angle fraction is 1.25×10^{-6} . The recoil electron distribution has a peak with widths of about 6° and 0.5 MeV, but the peak represents only about 15% of the total cross section. Thus, according to Figure 1, Compton conversion into the collimated peak has an efficiency of about $10^{-3} e^-/\gamma$. The sector magnet should be able to collect this beam with an efficiency greater than 10%. Combining these factors gives an overall

FIGURE 2. A simple 30° deflection sector dipole magnet can collect recoil electrons efficiently. The non-normal angle of incidence acts as an out-of-plane cylindrical lens to enhance electron collection. (08-00-1198-2238pb01)

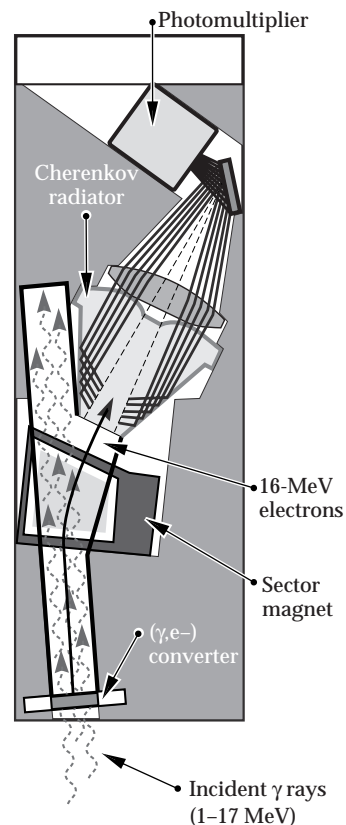
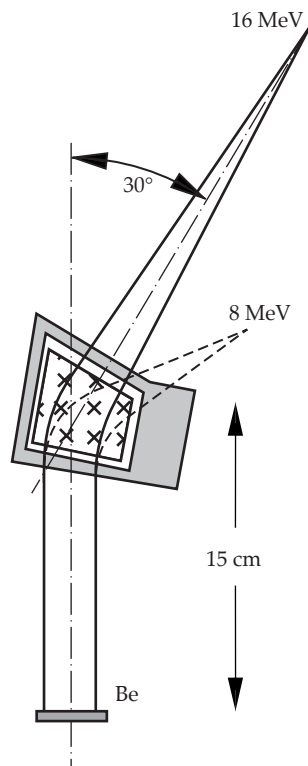


FIGURE 3. The overall FUDGE assembly can be compact. Here, a photomultiplier detects Cherenkov photons from energy-selected Compton electrons. The Cherenkov radiator is not exposed directly to the source, and “sees” only the deflected electrons. The photomultiplier is shielded heavily from the incident γ rays. (08-00-1198-2239pb02)

efficiency of about 1.25×10^{-10} electrons/16.7-MeV γ . This result can be used to determine the viability of the diagnostic. The system can produce a useful signal only if there is a statistically significant number of electrons. If we take 100 as the minimum number of electrons that can provide a measure of burn width, then the diagnostic is viable for (D,T) fusion neutron yields greater than about 10^{16} .

The nature of the signal depends on the method used to detect the electrons. A Cherenkov radiator optimized for electrons in this energy range can produce more than 500 visible photons per electron.¹¹ If the photons are detected with a fast MCP, then the signal will be a current pulse that can be recorded. Figure 3 illustrates a compact design for a FUDGE diagnostic with a microchannel plate (MCP) as the photodetector. With 100 electrons, an MCP gain of 10, a pulse width of 500 ps, the pulse will have a peak of about 2 A. This value seems very large for the signal, but it still represents only 100 initial Compton electrons. MCP response times today can be as short as 140 ps (Ref. 12), so burn widths of a few hundred picoseconds can be recorded with this approach.

Higher-bandwidth data can be recorded with a streak camera, at some possible expense in sensitivity. The challenge with this approach is to image enough of the Cherenkov photons onto the streak-camera slit to have a statistically significant measurement. We can

estimate the overall system efficiency: assuming a photocathode efficiency of 10%, approximately 1000 photons must be imaged onto the slit. The assumption above provides 5×10^4 photons from the Cherenkov radiator, so the Cherenkov image must have a transport efficiency of about 0.2%. This efficiency is feasible with a 50- μm streak camera slit, $f/3$ optics, and a 1-cm beam of electrons incident on the Cherenkov cone. Thus, incorporation of a streak camera might not compromise the overall system efficiency.

The estimate above only demonstrates the feasibility of designing a diagnostic for high-bandwidth recording of a fusion γ -ray signal. This is a compound system with multiple convolved distributions, so detailed predictions of system performance are difficult to calculate. This is a case where, ultimately, the performance of a FUDGE diagnostic must be calibrated on well characterized γ -ray sources.

Conclusion

FUDGE will bring together several kinds of issues that relate to ICF development at the NIF. The FUDGE method will use the high yields of NIF experiments to provide high-bandwidth measurements of fusion reaction history. When compared with fusion-neutron diagnostics, FUDGE data also will represent new measurements of absolute fusion cross sections and branching ratios. In this way, FUDGE will contribute to the

optimization of performance in ICF experiments and also will help advance our knowledge of the underlying fusion cross sections. These experiments should be excellent examples of doing science at the NIF.

Notes and References

1. R. A. Lerche, D. W. Phillion, and G. L. Tietbohl, *Rev. Sci. Instr.* **66**, 933 (1995).
2. J. E. Kammeraad, J. Hall, K. Sale, C. A. Barnes, S. E. Kellogg, T. R. Wang, et al., *Phys. Rev. C* **47**, 29 (1993).
3. S. S. Medley, A. L. Roquemore, and F. E. Cecil, *Rev. Sci. Instr.* **63**, 4857 (1992), and references therein.
4. M. J. Moran, *Rev. Sci. Instr.*, **56** 1067 (1985).
5. K. W. Wenzel, R. D. Petrasso, D. H. Lo, C. K. Li, J. W. Coleman, and J. R. Lierzer, *Rev. Sci. Instr.* **63**, 4840 (1992).
6. R. A. Lerche, M. D. Cable, and P. G. Dendooven, 12th International Conference on Laser Interaction and Related Phenomena, Osaka, Japan, (1995), and R. A. Lerche and M.D. Cable, *ICF Quarterly Report* **6**(3), 115, Lawrence Livermore National Laboratory, Livermore, CA, UCRL-LR-105821-96-3 (1996).
7. R. L. Gluckstern and M. H. Hull, Jr., *Phys. Rev.* **90**, 1030 (1953).
8. A. T. Nelms, *National Bureau of Standards Circular* 542 (1953).
9. L. Pages, E. Bertel, H. Joffre, and L. Sklavenitis, *Atomic Data* **4**, 1 (1972).
10. E. Segrè, *Experimental Nuclear Physics*, **1**, John Wiley & Sons (1953).
11. K.-P. Lewis, M. J. Moran, and J. Hall, *Rev. Sci. Instr.* **63**, 1988 (1992).
12. We have demonstrated this response time with measurements of a subpicosecond laser using a Hamamatsu 2566 MCP and Tektronix SCD5000 transient digitizer.